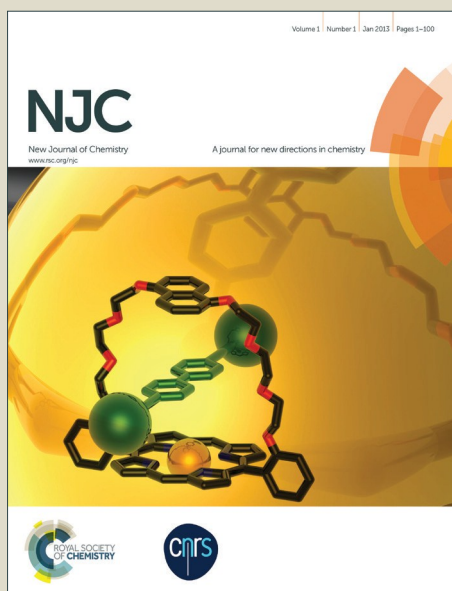


# NJC

Accepted Manuscript



This article can be cited before page numbers have been issued, to do this please use: D. Das, S. Adhikari, S. Lohar, B. Kumari, A. Banerjee, R. Bandopadhyay and J. Sanmartin, *New J. Chem.*, 2016, DOI: 10.1039/C6NJ02193J.



This is an *Accepted Manuscript*, which has been through the Royal Society of Chemistry peer review process and has been accepted for publication.

*Accepted Manuscripts* are published online shortly after acceptance, before technical editing, formatting and proof reading. Using this free service, authors can make their results available to the community, in citable form, before we publish the edited article. We will replace this *Accepted Manuscript* with the edited and formatted *Advance Article* as soon as it is available.

You can find more information about *Accepted Manuscripts* in the [Information for Authors](#).

Please note that technical editing may introduce minor changes to the text and/or graphics, which may alter content. The journal's standard [Terms & Conditions](#) and the [Ethical guidelines](#) still apply. In no event shall the Royal Society of Chemistry be held responsible for any errors or omissions in this *Accepted Manuscript* or any consequences arising from the use of any information it contains.

Cite this: DOI: 10.1039/c0xx00000x

www.rsc.org/xxxxxx

ARTICLE TYPE

## Cu(II) complex of a new isoindole derivative: structure, catecholase like activity, antimicrobial properties and bio-molecular interactions

Sangita Adhikari,<sup>a</sup> Sisir Lohar,<sup>a</sup> Babli Kumari,<sup>a</sup> Aparna Banerjee,<sup>b</sup> Rajib Bandopadhyay,<sup>b</sup> Jesús Sanmartín Matalobos<sup>c\*</sup> and Debasis Das<sup>c\*</sup>

Received (in XXX, XXX) XthXXXXXXXXX 20XX, Accepted Xth XXXXXXXXXXXX 20XX

DOI: 10.1039/b000000x

An isoindole based Cu(II) complex, [Cu(PICPH)Cl<sub>2</sub>] have been synthesized *in situ* by reacting copper(II) chloride with pyridine derived ligand, PICPH. The complex is characterized by spectroscopic techniques while its structure is confirmed by single crystal X-ray diffraction analysis. The complex has a trigonal bipyramid geometry containing both five- and seven member chelate rings. It shows catecholase like activity. Interaction of the complex with bio-relevant antipyrene derivative (ANNAP) is studied using fluorescence spectroscopy. DFT studies unfold the energetics associated with PICPH, [Cu(PICPH)Cl<sub>2</sub>] and the adduct between [Cu(PICPH)Cl<sub>2</sub>] and ANNAP. Antimicrobial activities of the compounds have also been studied.

**Introduction**

Isoindole, a member of fused benzopyrroles is known over a century. However, Nan'ya et al.<sup>1</sup> have developed a high yield method for its synthesis in a mixture of several other derivatives, the share of which depends on the nature of primary amine used, in addition to *o*-phthaldehyde. Five or six membered N-heterocyclic compounds have promising biological activities.<sup>2</sup> Being bioactive, isoindole derivatives are used as anti-viral, anti-cancer,<sup>3</sup> anti-inflammatory, organic dyes,<sup>4</sup> antitumor agent<sup>5,6</sup> and thrombin inhibitor.<sup>7</sup> Copper complex of bis-(2-pyridylimino)isoindoles show enantio-selective catalysis<sup>8</sup> for oxygenation of flavonol to *o*-benzoysalicylic acid.<sup>9</sup> It has photo physical application<sup>10</sup> and useful for catalytic hydrogenation.<sup>11,12</sup> Isoindole derivatives are key constituents of several bio-active natural products like jantine and the benzazepine alkaloid lennoxamine. Being unstable and reactive intermediate,<sup>13</sup> some isoindole derivatives are difficult to isolate and require *in situ* preparation.<sup>14</sup> It appears from literature that a wide area remains uncovered on the studies of isoindole based Cu(II) complexes. Hence, an isoindole based Cu(II) complex, [Cu(PICPH)Cl<sub>2</sub>] has been prepared, characterised and studied its properties in detail.

On the other hand, antipyrene and its derivatives have several biological applications.<sup>15</sup> 4-Aminoantipyrene protects against oxidative stress and acts as prophylactic for several diseases including cancer. Moreover, it's interesting structural features motivated researchers to study its coordination chemistry<sup>16,17</sup> Schiff bases of 4-aminoantipyrene and their metal complexes have biological,<sup>18</sup> clinical,<sup>19</sup> analytical,<sup>20</sup> anthelmintic, insecticidal,<sup>21</sup> and pharmacological<sup>22</sup> applications. 4-Aminoantipyrene is an intermediate of antipyretic and analgesic drugs.<sup>23</sup> These inspired us to prepare a new antipyrene derivative, ANNAP and study its antimicrobial activity for wide range of micro-organisms *viz.* *Escherichia coli*, *Pseudomonas sp.* *Staphylococcus aureus* or *Candida albicans* (fungus). In addition,

antimicrobial activities of [Cu(PICPH)Cl<sub>2</sub>] and its mixture with ANNAP have also been investigated by agar cup method<sup>24</sup> for comparison.

Additionally, the mutual interaction between ANNAP and [Cu(PICPH)Cl<sub>2</sub>] have been investigated by fluorescence and absorption spectroscopy.

It is well known that the active site of catechol oxidase<sup>25</sup> consists of a hydroxo bridged dicopper(II) centre where each Cu(II) centre is coordinated to three histidine nitrogen to adopt nearly trigonal pyramid (tbp) environment with one apical nitrogen. Mononuclear Cu(II) complex having intermediate geometry between tbp and square pyramid<sup>26</sup> is a potential model for catecholase activity.<sup>27</sup> These facts insisted us to investigate the catecholase activity of [Cu(PICPH)Cl<sub>2</sub>]. So far we are concerned, isoindole based Cu(II) complex having catecholase like activity is rare.

**Result and discussion****Single crystal X-ray structure of [Cu(PICPH)Cl<sub>2</sub>]**

The ORTEP of the asymmetric unit of [Cu(PICPH)Cl<sub>2</sub>] (Fig. 1) reveals a trigonal bipyramid geometry. The Cu(II) center is coordinated by three nitrogen atoms of the PICPH ligand and two chloride ions. In [Cu(PICPH)Cl<sub>2</sub>], chloride ions (Cl2 and Cl3) and imine nitrogen of PICPH (N20) occupy the equatorial positions whereas pyridine nitrogens (N13 and N23) occupy the apical positions. The complex has both five- and seven-member chelate rings. Its selected bond distances and angles are presented in Table S1 (see ESI). The Cu(1)–N(13) and Cu(1)–N(23), bond lengths are 2.011(2) and 1.985(2) Å, respectively, whereas the Cu(1)–Cl(2), Cu(1)–Cl(3) and Cu(1)–N(20) bond lengths are 2.2973(7), 2.4117(7) and 2.1446(19)Å, respectively. It is to be noted that Cu(1)–N(20) bond distance is significantly higher than Cu(1)–N(13) and Cu(1)–N(23) bond lengths. Besides, Cu(1)–Cl(3) bond length is higher than Cu(1)–Cl(2). Head-to-tail

stacked rings are responsible for their interactions within the crystal packing.

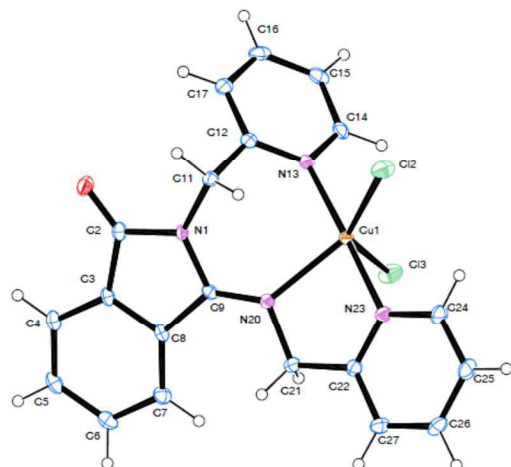


Fig. 1 ORTEP view of  $[\text{Cu}(\text{PICPH})\text{Cl}_2]$

### 5 Electron Paramagnetic Resonance (EPR) spectroscopy of $[\text{Cu}(\text{PICPH})\text{Cl}_2]$

X-band EPR spectra of  $[\text{Cu}(\text{PICPH})\text{Cl}_2]$  at two different temperatures, *viz.* 298K and 100K are shown in Fig.2. The *g* values are calculated using the equation,  $g = 0.71447752 \times \nu/H$  where  $\nu = 9.443\text{GHz}$ ,  $H = \text{field strength}$ . Thus, *g* values derived from the EPR spectra are collected in Table 1. The trend,  $g_{\parallel} > g_{\perp} > 2.0023$  indicates that unpaired electron resides at anti-bonding  $\psi_{\text{blg}}$  molecular orbital. It also indicates an elongated tetragonal bipyramid geometry around Cu(II), also corroborated from X-ray data.<sup>28</sup>

Table 1 EPR results of  $[\text{Cu}(\text{PICPH})\text{Cl}_2]$  at two different temperatures

$[\text{Cu}(\text{PICPH})\text{Cl}_2]$	$g_{\parallel}$	$g_{\perp}$	$g_{\text{av}}$
298K	2.2376	2.1457	2.1913
100K	2.2185	2.1468	2.1826

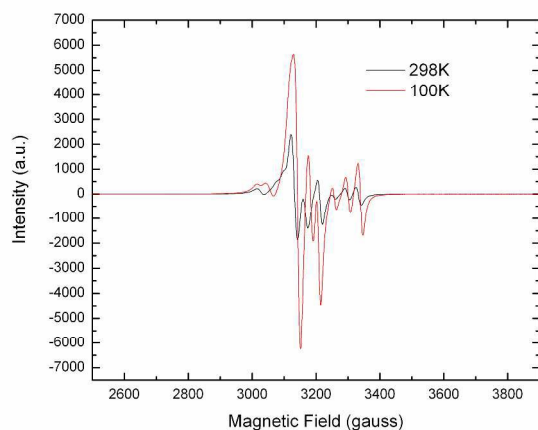


Fig.2 X-band EPR spectra of  $[\text{Cu}(\text{PICPH})\text{Cl}_2]$  at 298K and 100K

### Studies on interaction between $[\text{Cu}(\text{PICPH})\text{Cl}_2]$ and ANNAP by fluorescence and absorption spectroscopy

- 25 Free ANNAP shows emission at 462 nm, attributed to the excimer emission of naphthalene unit. Gradual addition of  $[\text{Cu}(\text{PICPH})\text{Cl}_2]$  diminishes the emission intensity, indicating their interaction. The quenching of emission intensity is probably due to paramagnetic effect of Cu(II) (Fig. 3).
- 30  $[\text{Cu}(\text{PICPH})\text{Cl}_2]$  shows absorbance at 223 nm and 256 nm, attributed to intra-ligand transitions. Gradual addition of ANNAP results a new absorption band at 350 nm, characteristics of ANNAP (Fig.3). Reverse addition, *i.e.* addition of  $[\text{Cu}(\text{PICPH})\text{Cl}_2]$  to ANNAP diminishes the absorbance at 350 nm, indicating significant interaction (Fig. 4). The formation of adduct between  $[\text{Cu}(\text{PICPH})\text{Cl}_2]$  and ANNAP is reflected from the molecular ion peak at *m/z*, 732.17 (Fig. S1, ESI).

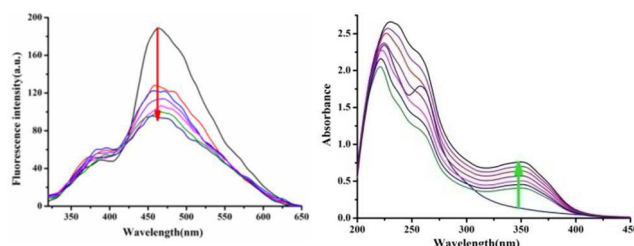
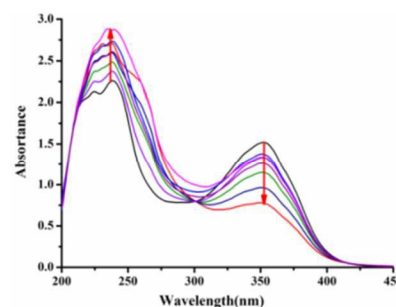


Fig. 3 Changes in the (a) emission profile of ANNAP (10 mM,  $\text{CH}_3\text{OH}$ ) upon gradual addition of  $[\text{Cu}(\text{PICPH})\text{Cl}_2]$  (10–100  $\mu\text{M}$ ) (left) and (b) absorption profile of  $[\text{Cu}(\text{PICPH})\text{Cl}_2]$  (10 mM,  $\text{CH}_3\text{OH}$ ) upon gradual addition of ANNAP (10–100  $\mu\text{M}$ ) (right).



40 Fig. 4 Changes in the absorbance of ANNAP (10 mM,  $\text{CH}_3\text{OH}$ ) upon gradual addition of  $[\text{Cu}(\text{PICPH})\text{Cl}_2]$  (10–100  $\mu\text{M}$ ).

### Catechol oxidase activity studies

- The 3,5-di-*tert*-butylcatechol (DTBC) is widely used among 45 different catechols available for catechol oxidase model studies. This is due to its low redox potential allowing easy oxidation to corresponding highly stable quinone (DTBQ) having maximum absorbance at 401 nm in methanol<sup>29</sup> whereas only  $[\text{Cu}(\text{PICPH})\text{Cl}_2]$  shows band only at 220 and 250 nm. For this 50 purpose,  $1 \times 10^{-4} \text{ mol dm}^{-3}$  solution of  $[\text{Cu}(\text{PICPH})\text{Cl}_2]$  is treated with  $1 \times 10^{-2} \text{ mol dm}^{-3}$  (100 equivalents) of DTBC under aerobic condition in methanol. A new absorption band that appears at 401nm increases with time while the solution color turns brown, indicating formation of quinone (Fig. 5).

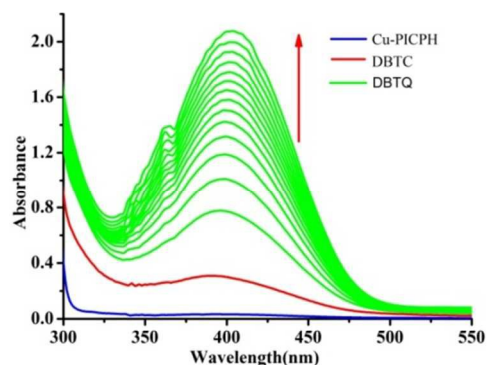


Fig. 5 Increase in the quinone absorbance (401 nm) upon addition of DTBC ( $1 \times 10^{-2}$  M) to the methanol solution of  $[\text{Cu}(\text{PICPH})\text{Cl}_2]$  ( $1 \times 10^{-4}$  M). The spectra are recorded at 5 min interval.

Kinetics of DTBC oxidation is monitored by absorption spectroscopy at  $25^\circ\text{C}$ . Keeping the concentration of  $[\text{Cu}(\text{PICPH})\text{Cl}_2]$  fixed at  $1 \times 10^{-4}$  mol  $\text{dm}^{-3}$ , the concentration of substrate (DTBC) is varied from  $1 \times 10^{-3}$  mol  $\text{dm}^{-3}$  to  $1 \times 10^{-2}$  mol  $\text{dm}^{-3}$ . For instance, 2 mL of DTBC solution of a particular concentration is quickly mixed to 0.04 mL of  $1 \times 10^{-3}$  mol  $\text{dm}^{-3}$   $[\text{Cu}(\text{PICPH})\text{Cl}_2]$  solution so that final concentration of Cu(II) complex becomes  $1 \times 10^{-4}$  mol  $\text{dm}^{-3}$ . At low concentration of DTBC, a first order dependence on substrate concentration is observed, however at higher concentrations saturation kinetics is followed. The plot of  $\log [A_t / (A_\infty - A_t)]$  vs. time generates the rate constant, provided in Table S2 (ESI).

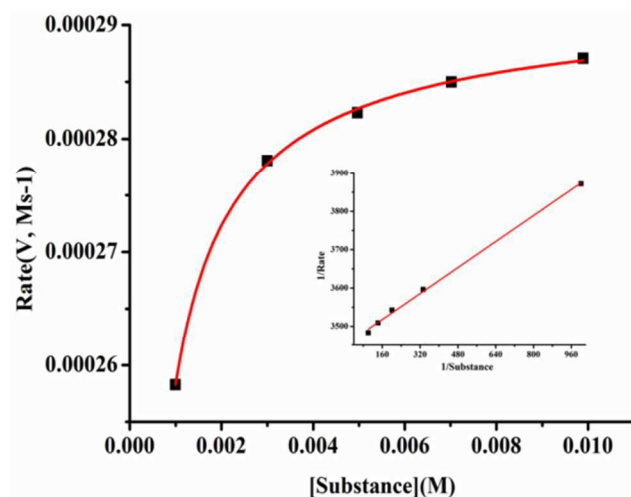


Fig. 6 Rate vs. substrate concentration plot for  $[\text{Cu}(\text{PICPH})\text{Cl}_2]$ . Inset: Lineweaver–Burk plot

Michaelis–Menten approach of enzymatic kinetics is then applied to analyse the results leading to Lineweaver–Burk (double reciprocal) plot (Fig. 6). The binding constant ( $K_M$ ), maximum velocity ( $V_{\text{max}}$ ), and rate constant (i.e., turn over number,  $k_{\text{cat}}$ ) are calculated from the Lineweaver–Burk plot following the equation,  $1/V = \{K_M/V_{\text{max}}\} \times \{1/[Subs]\} + 1/V_{\text{max}}$ . The values for  $k_{\text{cat}}$  are evaluated by applying the equation  $k_{\text{cat}} = (V_{\text{max}}/[Subs])$ . The kinetic parameters are presented in Table 2. The value of  $K_{\text{cat}}$ ,  $1.04 \times 10^4$  is comparable to the reported values.<sup>30–32</sup>

Table 2 Kinetic parameters associated with catecholase like activity of  $[\text{Cu}(\text{PICPH})\text{Cl}_2]$

Complex	Solvent	$V_{\text{max}}$ ( $\text{Ms}^{-1}$ )	$K_M$ (M)	$k_{\text{cat}}$ ( $\text{h}^{-1}$ )
$[\text{Cu}(\text{PICPH})\text{Cl}_2]$	Methanol	$2.90 \times 10^{-4}$	$1.22 \times 10^{-4}$	$1.04 \times 10^4$

The ESI-MS mass spectrum of the mixture of Cu(II) complex and DTBC (1: 100, mole ratio) throw some light on the probable mechanism of the catalytic reaction. The mass spectrum (Fig. S2, ESI) indicates a 1: 1 adduct between DTBC and Cu(II) complex ( $m/z = 630$ ). The peaks at  $m/z = 243$  and  $m/z = 352$  are assigned to quinone,  $[\text{DTBQ-Na}]^+$  and free ligand respectively. Copper complex exhibits the value of  $m/z = 463$ .

#### DFT studies

Density functional theoretical (DFT)<sup>33</sup> calculations (6-31G basis set) are used to optimize the energies and geometries<sup>34</sup> of PICPH, its Cu(II) complex, ANNAP and its adduct with the Cu(II) complex. Highest occupied and lowest unoccupied molecular orbitals i.e. HOMO and LUMO of the adduct (Fig. 7) indicates that most of the charge in HOMO resides on the heterocyclic ring of PICPH and ANNAP. HOMO–LUMO energy gaps in PICPH, its Cu(II) complex, ANNAP and its adduct with the Cu(II) complex are 0.164eV, 0.119eV, 0.134eV and 0.023eV respectively.

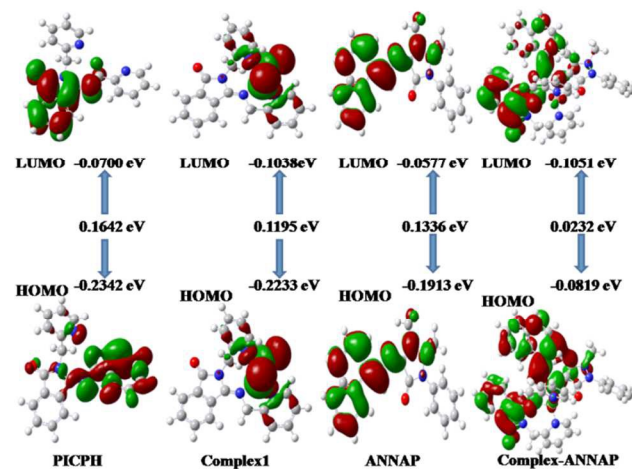


Fig. 7 HOMO–LUMO energies of PICPH,  $[\text{Cu}(\text{PICPH})\text{Cl}_2]$ , ANNAP and its adduct with  $[\text{Cu}(\text{PICPH})\text{Cl}_2]$ .

#### Electrochemical studies

The cyclic voltammogram of  $[\text{Cu}(\text{PICPH})\text{Cl}_2]$  (Fig.S3, ESI) in methanol displays one irreversible couple having  $E_{1/2}$ , +0.278 V, probably due to  $\text{Cu}^+/\text{Cu}^0$  couple. Another reversible couple with  $E_{1/2}$ , -0.149V may be due to  $\text{Cu}^{2+}/\text{Cu}^+$  couple.

The cyclic voltammogram of  $[\text{Cu}(\text{PICPH})(\text{Cl}_2)]$ -catechol system, recorded after 1h of mixing shows one quasi reversible couple with  $E_{1/2}$ , -0.067V.

#### Antimicrobial activity

$[\text{Cu}(\text{PICPH})\text{Cl}_2]$  and ANNAP are tested separately on some bacteria and fungi samples (Fig. S4, ESI). No significant *in vitro* antibacterial activity has been observed against *Pseudomonas fluorescens* and *Bacillus anthracis*. Similarly *in vitro* antifungal activity is absent against *Trichoderma viride*. MIC reveals that their mixture has better biological activity (Fig. 8) than individual

compounds. The antibacterial and antifungal properties of the mixed system is good enough compared to some recent reports.<sup>35</sup>

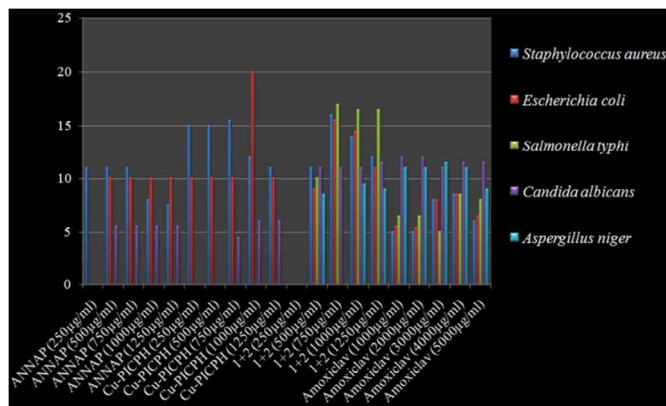


**Fig 8** Minimum inhibitory concentrations (MIC) of the tested compounds against gram negative *E.coli* and *Salmonella typhi*, gram positive *Staphylococcus aureus* and fungi *C.albicans* and *A.niger*.

### Thermogravimetric analysis (Fig. S5, ESI)

The complex undergoes four steps decomposition from 30 to 750°C. During first step (30-159)°C, loss of one chlorine atom corresponds to 92.40% wt. loss (calcd. value, 92.67%). In the temperature region, from 159 to 470°C, another chlorine atom, a carbonyl group, a benzene moiety and two carbon atoms are lost leading to 52.89% wt. loss (calcd. value, 53.23%). Finally, it loses 17.23% wt. (calculated value, 17.09%) in the temperature region 470 to 750 °C, keeping behind, CuO.

### Conclusion

Herein a simple route for synthesis of a new isoindole based Cu(II) complex, [Cu(PICPH)Cl<sub>2</sub>] is reported. The complex is characterized by single crystal X-ray diffraction analysis. It has trigonal bipyramid geometry with both five- and seven member chelate rings. The complex shows significant catecholase like activity associated with  $K_{cat} = 1.04 \times 10^4$ . Electron paramagnetic resonance studies on the complex reveals the g value. Spectroscopic interactions of the complex with bio-relevant newly synthesised antipyrine derivative (ANNAP) have also been investigated. DFT studies unfold the energetics associated with PICPH, [Cu(PICPH)Cl<sub>2</sub>] and the adduct between [Cu(PICPH)Cl<sub>2</sub>] and ANNAP. Antimicrobial activities of the compounds are very promising. Thus, the present studies opens up a new direction in isoindole based copper chemistry with potential bio-medical application.

### Experimental

#### Materials and methods

All reagents and solvents are of A. R. grade and used without further purification. Copper(II) chloride, 4-amino antipyrine, *o*-phthaldehyde, picolyl amine are purchased from Sigma Aldrich (India). Milli-Q 18.2 MΩ cm<sup>-1</sup> water is used throughout all the experiments. <sup>1</sup>H NMR spectra are recorded using Bruker Advance DPX 400 (400 MHz) in CDCl<sub>3</sub>. A Shimadzu Multi Spec 1501 spectrophotometer is used for recording UV-Vis spectra. FTIR spectra are recorded on a PerkinElmer FTIR (model RX1) spectrometer on KBr pellet. Electrochemical experiments have

been performed in dry acetonitrile solution under nitrogen atmosphere using 0.1 M TBAP as supporting electrolyte. The instrument (CHI620D potentiometer) is equipped with three-electrode system: a platinum disk working electrode, a platinum wire auxiliary electrode and a calomel reference electrode. All potentials have been determined at a scan rate of 100 mV s<sup>-1</sup> at room temperature. Thermal analyses have been performed with a Perkin-Elmer Diamond TG/DT analyzer in the temperature ranging 30°C to 700°C under nitrogen. Steady state fluorescence is measured using Hitachi F-4500 spectrofluorimeter.

### X-ray diffraction data

Single crystal X-ray diffraction data for [Cu(PICPH)Cl<sub>2</sub>] are collected at 100(2) K, on a Bruker X8 kappa APEXII CCD diffractometer using graphite-monochromated Mo-Kα radiation ( $\lambda = 0.71073 \text{ \AA}$ ). Data are processed and corrected for Lorentz and polarization effects. Selective cell parameters are presented in Table S3, ESI. Multi-scan absorption corrections were performed using the SADABS routine.<sup>36</sup> Structures were solved by standard direct methods using SIR2004,<sup>37</sup> and then were refined by full matrix least squares on  $F^2$  using SHELXL97.<sup>38</sup> SQUEEZE/PLATON was used in structural refinement. All non-hydrogen atoms are anisotropically refined. Hydrogen atoms are included in the structure factor calculation in geometrically idealized positions, with thermal parameters depending of the parent atom, by using a riding model. The selected bond lengths and angles are presented in Table S3 (ESI).

### EPR measurements

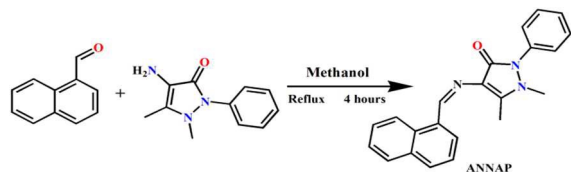
X-Band EPR measurements have been performed with a Bruker EMX EPR spectrometer. Sample is placed into quartz EPR tube and spectra are acquired both at room and liquid nitrogen temperatures, using a power of 1.006 mW. In general, the spectra obtained from 83.886s scans with 500 to 6000 Gauss, time constant of 10.240 ms, modulation amplitude of 4.00 Gauss, and field modulation frequency of 100.00 kHz.

### Synthesis of [Cu(PICPH)Cl<sub>2</sub>]

15 mL ethanol solution of picolyl amine (0.107g, 1 mmol) is added to 10 mL solution of *o*-phthaldehyde (0.268g, 2mmol) in ethanol and refluxed for 4 h. The ESI-MS spectrum of the mixture indicates formation of the major product, 1:1 Schiff base along with some unidentified molecules. ESI-MS (m/z): [M+Na]<sup>+</sup> 247.11 (calcd. 247.67) (Fig. S6, ESI). However, addition of methanol solution of copper(II) chloride (0.034g, 0.2 mmol, 10 mL) to this mixture under stirring condition turned the solution deep green that resulted single crystal X-ray diffraction quality crystals after 7 days. FTIR (ν, cm<sup>-1</sup>): 3332, 3214 and 1600 (Fig. S7, ESI). ESI-MS (m/z): 391.13 calcd. 391.15 (Fig.S8, ESI). Thermogram is presented in Fig.S5 (ESI).

### Synthesis of ANNAP

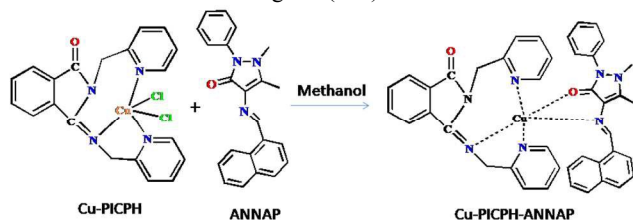
ANNAP has been synthesised by refluxing equimolar mixture of 4-amino antipyrine and *o*-naphthaldehyde in methanol for 6h (Scheme 1). The brown-yellow solid is obtained after slow evaporation of the solvent. Yield is 85%. ESI-MS (m/z): 341.13, calcd. 341.15 (Fig. S9, ESI), FTIR (ν, cm<sup>-1</sup>): 3332, 3214 and 1600 (Fig. S10, ESI), <sup>1</sup>H NMR (400 MHz, CDCl<sub>3</sub>, Fig. S11, ESI) 2.6 (3H, s), 3.2 (3H, s), 7.3 (1H, s), 7.4 (2H, d, J = 7.2Hz), 7.5 (2H, 8Hz), 7.6 (3H, d, J = 8.13Hz), 8.0 (2H, d, 8.4Hz), 8.2 (1H, 6.8), 8.9 (1H, 8.4), 10.6 (1H, s).



Scheme 1 Synthesis of ANNAP

**Synthesis of ANNAP-[Cu(PICPH)Cl<sub>2</sub>] adduct**

The adduct has been synthesised by stirring equimolar mixture of ANNAP and Cu-PICPH in methanol for 1h (Scheme 2). ESI-MS spectrum shows peak at m/z, 732.17 indicating probable structure of the adduct as shown in Fig. S1 (ESI).



Scheme 2 Synthesis of ANNAP- Cu(PICPH) adduct

**Antimicrobial activity**

ANNAP, [Cu(PICPH)Cl<sub>2</sub>] and their mixture are screened for *in vitro* antimicrobial activities against two Gram-negative (*Escherichia coli* NCIM 2832 and *Salmonella typhi* NCIM 2501), one Gram-positive (*Staphylococcus aureus* NCIM 2122) bacteria and fungi (*Candida albicans* NCIM 3471, *Trichoderma viride* NCIM 122 and *Aspergillus niger* NCIM 1056) by agar cup method. Culture media for bacteria Mueller Hinton agar and for fungi potato dextrose agar are poured into sterile petriplates and microorganisms are spread on the agar plate surface using a sterile cotton swab individually. Standard drug amoxiclav is taken as positive control and distilled water as negative control on each plate. The plates are incubated at 37°C (24 h) and 30°C (48 h) for bacterial and fungal strains respectively. The minimum inhibitory concentration (MIC) for each compound was checked by zone of inhibition calculation (mm).

**Acknowledgements**

S. Adhikari, B. Kumari and A. Banerjee are grateful to Department of Environment (Govt. W. B.) and BU for fellowship.

**Notes and references**

CCDC of the complex is 927870.

<sup>a</sup>Department of Chemistry, The University of Burdwan, Burdwan, West Bengal, India

<sup>b</sup>Department of Botany, The University of Burdwan, Burdwan, West Bengal, India

<sup>c</sup>Departamento de Quimica Inorganica, Facultad de Quimica, Avda. Das Ciencias s/n, 15782 Santiago de Compostela, Spain.

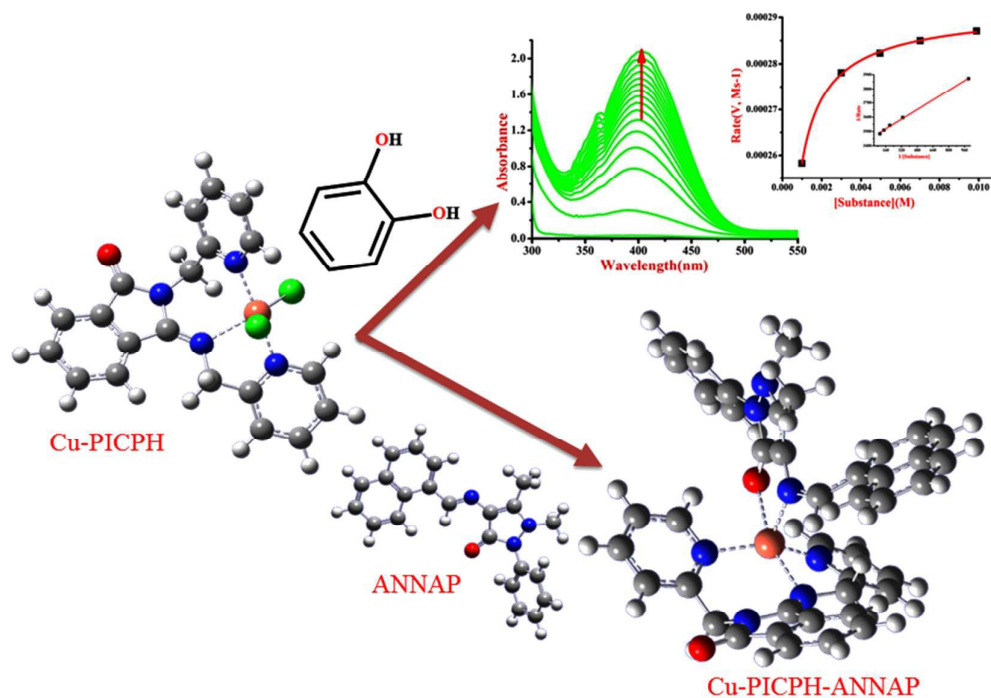
† Electronic Supplementary Information (ESI) available: See DOI: 10.1039/b000000x/

- (a) S. Nan'ya, T. Tange and E. Maekawa, *J Heterocycl. Chem.*, 1985, **22**, 449.

- (a) D. R. Korakas and G. Varvounis, *J. Heterocycl. Chem.*, 1994, **31**, 1317. (b) P. Barraja, V. Spanò, D. Giallombardo, P. Diana, A. Montalbano, A. Carbone, B. Parrino and G. Cirrincione, *Tetrahedron*, 2013, **69**, 6474.
- B. Parrino, A. Carbone, V. Spanò, A. Montalbano, D. Giallombardo, P. Barraja, A. Attanzio, L. Tesoriere, C. Sissi, M. Palumbo, G. Cirrincione and P. Diana, *Eur. J. Med. Chem.*, 2015, **94**, 367.
- (a) K. Speck and T. Magauer, *Beilstein J. Org. Chem.* 2013, **9**, 2048.
- T. S. A. Heugebaert, B. I. Roman and C. V. Stevens, *Chem. Soc. Rev.*, 2012, **41**, 5626.
- Q. Ding, B. Wang and J. Wu, *Tetrahedron Lett.*, 2007, **48**, 8599. (b) A. Carbone, B. Parrino, G. Di Vita, A. Attanzio, V. Spanò, A. Montalbano, P. Barraja, L. Tesoriere, M. A. Livrea, P. Diana and G. Cirrincione, *Marine Drugs*, 2015, **13**, 460.
- D.-R. Hou, M.-S. Wang, M.-W. Chung, Y.-D. Hsieh and H.-H. G. Tsai, *J. Org. Chem.*, 2007, **72**, 9231.
- (b) B. K. Langlotz, H. Wadeplahl and L. H. Gade, *Angew. Chem. Int. Ed.*, 2008, **47**, 4670.
- Ä. B. Hergovich, J. Kaizer, G. Speier, G. Huttner and A. Jacobi, *Inorg. Chem.*, 2000, **39**, 4224.
- H.-M. Wen, Y.-H. Wu, Y. Fan, L.-Y. Zhang, C.-N. Chen and Z.-N. Chen, *Inorg. Chem.*, 2010, **49**, 2210.
- (a) J. S. Pap, B. Kripli, T. Varadi, M. Giorgi, J. Kaizer and G. Speier, *J. Inorg. Biochem.*, 2011, **105**, 911; (b) J. Kaizer, T. Csay, P. Kovari, G. Speier and L. Parkanyi, *J. Mol. Catal. A: Chem.*, 2008, **280**, 203.
- B. Siggelkow, M. B. Meder, C. H. Galka and L. H. Gade, *Eur. J. Inorg. Chem.*, 2004, 3424.
- (a) Z. H. Chen, P. Muller and T. M. Swager, *Org. Lett.*, 2006, **8**, 273; (b) B. Sadowski, J. Klajn and D. T. Gryko, *Org. Biomol. Chem.*, 2016, **14**, 7804.
- (a) Y.-L. Chen, M.-H. Lee, W.-Y. Wong and A. W. M. Lee, *Synlett.*, 2006, **15**, 2510; (b) Y. G. Shi, D. T. Yang, S. K. Mellerup, N. Wang, T. Peng and S. Wang, *Org. Lett.*, 2016, **18**, 1626.
- (a) J. Hosler, C. Tschanz, C. E. Hignite and D. L. Azarnoff, *J. Invest. Dermatol.*, 1980, **74**, 51; (b) K. Z. Ismail, A. El-Dissouky and A. Z. Shehada, *Polyhedron* 2009, **16**, 2909; (c) A. M. Farghaly, A. Hozza, *Pharmazie.*, 1980, **35**, 596. (c) M. Manjunath, A. D. Kulkarni, G. B. Bagihalli, S. Malladi and S. A. Patil, *J. Molec. Struc.*, 2017, **1127**, 314.
- E. Pontiki; D. H.-Litina; K. Litinas, O. Nicolotti, A. Carotti *Eur. J. Med. Chem.*, 2011, **46**, 200.
- (a) S. Rawther, M. R. Gopalakrishnan, *J. Indian Chem. Soc.* 1992, **69**, 117; (b) J. Dick, R. Bacaloglu, A. Maure, *Rev. Roum. Chim.*, 1967, **10**, 833.
- D. G. Craciunescu, *An. R. Acad. Farm.*, 1977, **43**, 256.
- J. Hosler, C. Tschanz, C. E. Hignite and D. L. Azarnoff, *J. Invest. Dermatol.*, 1986, 74951.
- N. L. Olenovich and L. I. Kovalchuk *Z. Anal. Kim.*, 1975, **28**, 2162.

21. M. Himaja, K.Rai, K. V. Anish, M. V. Ramana and A. A. Karigar, *J. Pharm. Sci. Innov.*, 2012, **1**(1), 67.
22. P. J. Meffin, R. Williams, T. F. Blaschke and M. Rowland, *J. Pharm. Sci.*, 1977, **66**, 135.
23. (a) E. E. Elemike, A. P. Oviawe and I. E. Otuokere, *Res. J. Chem. Sci.*, 2011, **1**(8), 6.(b) M. S. Alam and D. U. Lee, *J. Molecu. Struct.*, 2017, **1128**, 174.
24. (a) S. B. Rose and R. E. Miller, *J. Bacterial.*, 1939, **38**(5), 525; (b) B. Bonov, J. Hooper and J. Parisot, *J. Antimicrob. Chemother.*, 2008, **61**(6), 1295.(c) G. Kaur and S. Singh, *IJPSR*, 2016, **7**(5), 2057. (d) S. K. Panda, Y. K. Mohanta, L. Padhi, Y. H. Park, T. K. Mohanta and H. Bae, *Molecules*, 2016, **21**(3), 293.
25. E. I. Solomon, U. M. Sundaram and T. E. Mackonkin, *Chem. Rev.*, 1996, **96**, 2563.
26. G.C. Percy and J. Thornton, *J. Inorg. Nucl. Chem.*, 1973, **35**, 2319.
27. C.H. Kao, H.H. Wei, Y.H. Liu, G.H. Lee, Y. Wang and C.J. Lee, *J. Inorg. Biochem.*, 2001, **84**, 171.
28. F. Valach, N. Hoang, M. Dunaj-Jurčo and M. Mělník, *Proceedings of the 12th Conference on Coordination Chemistry*. Smolenice, 1989.
29. (a) E. I. Solomon, U. M. Sundaram and T. E. Machonkin, *Chem. Rev.*, 1996, **96**, 2563; (b) M. Winkler, K. Lerch and E. I. Solomon, *J. Am. Chem. Soc.*, 1981, **103**, 7001
30. S. Adhikari, A. Banerjee, S. Nandi, M. Fondo, J. S. Matalobos and D. Das, *RSC Adv.*, 2015, **5**, 10987.
31. K. S. Banu, T. Chattopadhyay, A. Banerjee, S. Bhattacharya, E. Suresh, M. Nethaji, E. Zangrando and D. Das, *Inorg. Chem.*, 2008, **47**, 7083.
32. F. Zippel, F. Ahlers, R. Werner, W. Haase, H.-F. Nolting and B. Krebs, *Inorg. Chem.*, 1996, **35**, 3409
33. Gaussian 03, Rev. C. 02, Gaussian Inc., Wallingford CT, 2004.
34. D. Karak, S. Das, S. Lohar, A. Banerjee, A. Sahana, I. Hauli, S. K. Mukhopadhyay, D. A. Safin, M. G. Babashkina, M. Bolte, Y. Garcia and D. Das, *Dalton Trans.*, 2013, 6708.
35. (a) A.A. Osowole and S.A. Balogun, *Europ.J. Appl. Sci.*, 2012, **4**(1), 6; (b) B. Shaabani, A. A. Khandar, M. Dusek, M. Pojarova, M. A. Maestro, R. Mukherjee and F. Mahmoudi, *J. Coord. Chem.*, 2014, **67**, 12, 2096; (c) N. C. Kasuga, K. Sekino, C.Koumo, N. Shimada, M. Ishikawa and K. Nomiya, *J. Inorg. Biochem.*, 2001, **84**, 55.
36. R. H. Blesing, *Acta. Cryst.*, 1995, **A51**, 33.
37. M. C. Burla, R. Caliandro, M. Camalli, B. Carrozzini, G. L. Cascarano, L. De Caro, C. Giacovazzo, G. Polidori and R. Spagna, *J. Appl. Cryst.*, 2005, **38**, 381.
38. G. M. Sheldrick, *Acta. Cryst.*, 2008, **A64**, 112.

## Table of contents



An isoindole based trigonal bipyramidal Cu(II) complex shows catecholase and antimicrobial activities. It interacts with bio-relevant antipyrine derivative.